1991

Cadmium Adsorption on Iron Oxides in the Presence of Alkaline-Earth Elements

Christina Cowan
Pacific Northwest National Laboratory

John M. Zachara
Pacific Northwest National Laboratory, john.zachara@pnl.gov

Charles T. Resch
Pacific Northwest National Laboratory

Environ. Sci. Technol. **1991**, *25*, 437–446

Cadmium Adsorption on Iron Oxides in the Presence of Alkaline-Earth Elements

Christina E. Cowan,* John M. Zachara, and Charles T. Resch

Environmental Sciences Department, Battelle, Pacific Northwest Laboratories, P.O. Box 999, MSIN K3-61, Richland, Washington 99352

■ Cadmium sorption on $Fe_2O_3 \cdot H_2O$(am) in the presence of alkaline-earth cations was investigated with emphasis on the Cd–Ca binary system. In binary-element sorption experiments with Ca, Mg, Sr, and Ba, competition was observed primarily in Cd–Ca binary mixtures, which were studied at three ionic strengths (0.5, 0.1, and 0.005 M). The extent of competition increased with increasing Ca concentration. In single-element experiments changes in ionic strength (between 0.005 and 0.5 M) did not influence Cd sorption but did affect Ca sorption, implying that a portion of the Ca surface complexes were outer sphere. The triple-layer model (TLM), using inner- and outer-sphere complexation reactions, and the nonelectrostatic model (NEM), incorporating only one adsorption plane, both adequately represented the adsorption of the individual elements and predicted the Cd–Ca competition at ionic strengths of 0.5 and 0.1 M. Neither model predicted the competition at 0.005 M. The NEM better simulated the shape of the measured Cd–Ca adsorption edge at all ionic strengths. The combined experimental and modeling results suggest that Cd–Ca competitive adsorption on $Fe_2O_3 \cdot H_2O$(am) occurs via mass action on mutually accessible surface sites.

Introduction

Transition metals bind strongly to both iron and manganese oxides (*1–7*). Sorption to these solids is thought to exert a major control on metal concentrations in surface waters, soils, and groundwaters (*8–12*). In natural water systems, metallic cations, such as Cd, Cu, and Zn, do not occur as single solutes but are more often found in combination with other metals and higher concentrations of alkaline-earth cations such as Ca^{2+} or Mg^{2+}. Therefore, accurate prediction of the extent of metal sorption onto oxides in soil or subsurface materials requires (1) an understanding of the competitive effects between these metal and alkaline-earth cations and (2) descriptive models that can accurately describe the observed presence or absence of competition.

Competitive adsorption between transition-metal cations has been observed on iron and aluminum oxides (*13*, *14*) and manganese oxides (*15*). In binary adsorption experiments with transition metals and cadmium, Benjamin and Leckie (*13*, *14*) found that the extent of competition depended on the specific combination of metal cations evaluated (e.g., Zn had a greater effect on Cd adsorption than either Cu or Pb did). They concluded that each of the metals was predominantly sorbing to different sites and that competition resulted when the metals adsorb to mutually compatible sites. Zasoski and Burau (*15*), in their evaluation of Zn and Cd binary adsorption on δ-MnO_2, also found that their results were best explained by the presence of two types of binding sites with different preferences for the two metals. Swallow et al. (*16*) were unable to determine whether competition occurred between Cu and Pb on amorphous iron oxyhydroxide [$Fe_2O_3 \cdot H_2O$(am)] because, for the concentrations evaluated, saturation of the surface was not achieved before the metal hydroxide solid phase formed.

The potential competitive effect of alkaline-earth elements on the sorption of transition metals has received limited attention, yet it may be important in soil solutions, groundwater, and other natural waters in which the dominant electrolyte cation is Ca or Mg. Dempsey and Singer (*17*) found that the presence of calcium significantly reduced the sorption of Zn on MnO_x but not on $Fe_2O_3 \cdot H_2O$(am). In a study of the adsorption of Cu, Pb, Zn, and Cd on goethite in artifical seawater, Balistrieri and Murray (*3*) determined that sorption of Mg on the surface of the goethite reduced the sorption of these other metals.

Surface-complexation models [as reviewed in Westall and Hohl (*18*) and Sposito (*9*)] have been widely used to describe metal ion sorption on oxide and oxide-like surfaces [for example, Stumm et al. (*19*), Davis and Leckie (*1*), and Hayes and Leckie (*20*)]. These surface-complexation models require knowledge of the properties of the oxide surface and assumptions about the location and form of the sorbed ions in the electrical double layer near the oxide surface. The models have been effective in simulating the sorption of elements from simple solutions; however, their applicability to modeling complex systems where elements in solution may compete with each other for sorption sites has received only limited attention (*3*, *21–23*).

The objective of the research described here was to determine whether the sorption of cadmium onto $Fe_2O_3 \cdot H_2O$(am) is affected by the presence of the alkaline-earth elements Mg, Ca, Sr, and Ba at concentrations representative of soil solutions and groundwaters. Using the sorption data, several alternative surface-complexation modeling approaches for describing the competition between the alkaline-earth elements and Cd on the $Fe_2O_3 \cdot H_2O$(am) were evaluated.

Experimental Procedures

All reagents were prepared in distilled, deionized water that was degassed by boiling and then sparging with prepurified N_2. The solution pH was adjusted in the adsorption experiments with HNO_3 (Ultrex) and with CO_2-free NaOH. The NaOH was stored under N_2 to prevent CO_2(g) adsorption.

A 10^{-2} M stock solution of Cd was prepared by dissolving $CdCl_2$ powder (Aldrich Gold Label) in deionized water. A 10-fold dilution was made to prepare the final 10^{-3} M Cd stock solution for the adsorption experiments. Carrier-free ^{109}Cd as $CdCl_2$ (New England Nuclear) was used as a radiotracer, and counting was performed by liquid scintillation. The concentration of the Cd in the stock solution was verified by inductively coupled plasma spectroscopy (ICP). Stock solutions of 7.5×10^{-2} M Ca^{2+}, 0.1 M Mg^{2+}, 5×10^{-2} M Sr^{2+}, and 5×10^{-2} M Ba^{2+} were prepared from their nitrate salts, and their absolute concentrations were confirmed by ICP.

Preparation of Amorphous Iron Oxyhydroxide. Amorphous iron oxyhydroxide [$Fe_2O_3 \cdot H_2O$(am)] suspensions were prepared under N_2 in water-jacketed, Pyrex flasks as described by Zachara et al. (*22*). The temperature of the suspension was maintained at 25 °C by water flowing through the jacket from a refrigerating/heating circulating bath. Carbonate-free conditions were main-

0013-936X/91/0925-0437$02.50/0

Table I. Triple-Layer Model Parameters for Amorphous Iron Oxyhydroxide

parameter	value	ref
surface site density (N_s)	11 sites/nm^2	1
surface area (S)	600 m^2/g	24
outer-layer capacitance (C_2)	0.20 F/m^2	1
inner-layer capacitance (C_1)	1.25 F/m^2	24

tained by using a glovebox with N_2 atmosphere or, more commonly, in a reaction flask with continuous N_2 sparging to prevent air intrusion. After preparation, the suspension containing 0.043 M Fe was allowed to equilibrate under N_2 atmosphere (25 °C) overnight (approximately 14 h) before use in the adsorption experiments. An aliquot of the suspension was removed, washed with water several times by centrifugation, and then lyophilized. The lyophilized sample was dissolved in concentrated HCl (Ultrex) and analyzed for Fe. The surface properties of amorphous iron oxide prepared by a similar method have been reported elsewhere (*1*, *22*) and are summarized in Table I.

Adsorption Edges. The fractional adsorption of cadmium (10^{-7} and 10^{-8} M) and calcium (0.027, 0.10, 0.20, 0.76, and 2.4 mM) on $Fe_2O_3{\cdot}H_2O$(am) was determined over a range of pH in 500-mL jacketed Pyrex flasks. Suspensions of $Fe_2O_3{\cdot}H_2O$(am) (~0.8 mM Fe) were established in the desired molarity of $NaNO_3$(aq) (0.1 M for Cd, and 0.5, 0.1, and 0.005 M for Ca). The suspension pH was adjusted with an automatic pH stat/titrimeter to the desired starting point between pH 4 and 6, depending on the sorbate and sorbent concentrations, and the suspension was then equilibrated for 1 h under N_2 with stirring. The appropriate amount of Cd stock solution was then added, yielding approximately 10 000 cpm of radiolabel/mL. Two 10-mL samples of the suspension were removed to N_2-purged centrifuge tubes, and the pH of the suspension was adjusted upward by approximately 0.5 pH unit with the pH stat/titrimeter. Duplicate samples were removed at each pH, and pH adjustment continued until the final pH was attained (pH 7–9 depending on the sorbate). The samples in centrifuge tubes were equilibrated with shaking under N_2 for 4 h at 25 °C. Time-course studies indicated that this length of time was adequate for the solutions to achieve steady state. The suspensions were then centrifuged at 4900 rcf at 25 °C, and the final pH was measured with a Ross combination electrode under N_2. Subsamples of the supernatant were placed in tared, acidified (with Ultrex HCl) vials for scintillation counting (glass vials) and ICP analysis (plastic vials).

For the competition experiments involving cadmium with each of the alkaline-earth elements, the $Fe_2O_3{\cdot}H_2O$(am) suspension described above was spiked with the appropriate amount of alkaline-earth (Ca, Mg, Ba, or Sr) stock solution and equilibrated for 1 h. A 10-mL subsample of the solution was removed and centrifuged at 4900 rcf for 20 min. The supernatant was then removed for ICP analysis of the alkaline-earth concentration. Appropriate amounts of electrolyte and Cd stock solutions were added and the experiments continued as described in the preceding paragraph. Competition was evaluated with Cd at 10^{-6} M and the alkaline-earth cations at various concentrations summarized in Table II. Care was taken in all the experiments to exclude CO_2(g)), which would otherwise cause the precipitation of the alkaline-earth carbonates. The M^{2+} concentrations were below the concentration at which either hydroxide or carbonate solids would form if the solutions were in equilibrium with atmospheric CO_2(g).

Desorption. To determine the effect of addition of various Ca concentrations on the desorption of Cd from $Fe_2O_3{\cdot}H_2O$(am), Cd was sorbed onto $Fe_2O_3{\cdot}H_2O$(am) by the method described for the adsorption edges. After the Cd had equilibrated with the $Fe_2O_3{\cdot}H_2O$(am) for 4 h, subsamples were removed for analysis to determine the adsorbed concentration. Calcium was added at concentrations of 0.25, 2.5, and 25 mM. Samples and pH measurements at each Ca concentration were taken after 24, 48, and 144 h. The samples were analyzed for Cd by scintillation counting, and Ca was measured by ICP.

Adsorption Modeling. Adsorption constants for the triple-layer model (TLM) representing the sorption of Cd and Ca individually on $Fe_2O_3{\cdot}H_2O$(am) were determined by using the program FITEQL (*25*, *26*) and the surface characteristics of $Fe_2O_3{\cdot}H_2O$(am) given in Tables I and III. Solution-complexation reactions and associated constants for Cd and the alkaline-earth elements are also given in Table III.

Adsorption constants for a nonelectrostatic site-binding model (NEM) for the sorption of Cd and Ca individually on $Fe_2O_3{\cdot}H_2O$(am) were also determined with the program FITEQL. This model treats the binding of metal ions to oxide surfaces as analogous to complexation with ligands in solution. The surface area and site densities given in Table I were used to represent the $Fe_2O_3{\cdot}H_2O$(am); the capacitances were not needed because this model contains no electrostatic terms. The acidity and electrolyte constants were determined by fitting them to potentiometric titration data (*27*) with FITEQL (Table III). The NEM fit to the potentiometric titration data was not quite as good

Table II. Experimental Conditions for Competition Experiments

	alkaline earth		transition metal			iron oxides	pH	
ref	element	concn, M	element	concn, M	ionic strength, M	concn, M	50%[a]	iron oxide
b	Mg	7.5×10^{-3}	Cd	1×10^{-6}	0.1 $NaNO_3$	0.87×10^{-3}	7.0	Fe(OH)(am)
b	Ca	2.5×10^{-3}	Cd	1×10^{-6}	0.1 $NaNO_3$	0.87×10^{-3}	7.3	Fe(OH)(am)
b	Ca	7.5×10^{-3}	Cd	$1. \times 10^{-6}$	0.1 $NaNO_3$	0.87×10^{-3}	7.3	Fe(OH)(am)
b	Ca	2.5×10^{-3}	Cd	1×10^{-6}	0.1 $NaNO_3$	0.80×10^{-3}	7.0	Fe(OH)(am)
b	Ca	2.5×10^{-3}	Cd	1×10^{-6}	0.5 $NaNO_3$	0.80×10^{-3}	6.9	Fe(OH)(am)
b	Ca	2.5×10^{-3}	Cd	1×10^{-6}	0.005 $NaNO_3$	0.80×10^{-3}	6.9	Fe(OH)(am)
b	Sr	5.1×10^{-4}	Cd	8.9×10^{-7}	0.1 $NaNO_3$	0.87×10^{-3}	6.7	Fe(OH)(am)
b	Ba	5.0×10^{-4}	Cd	8.9×10^{-7}	0.1 $NaNO_3$	0.87×10^{-3}	6.7	Fe(OH)(am)
b	Ba	1.0×10^{-3}	Cd	8.9×10^{-7}	0.1 $NaNO_3$	0.87×10^{-3}	6.7	Fe(OH)(am)
b	Sr	5×10^{-4}	Cd	8.9×10^{-7}	0.1 $NaNO_3$	0.87×10^{-4}	6.7	Fe(OH)(am)
b	Ba	1×10^{-3}	Cd	8.9×10^{-7}	0.1 $NaNO_3$	0.87×10^{-4}	6.7	Fe(OH)(am)
3	Mg	0.054	Zn	2.7×10^{-6}	0.53 NaCl + 0.054 $MgCl_2$	6.19×10^{-3}		γ-FeOOH
3	Mg	0.054	Cd	2.8×10^{-6}	0.53 NaCL + 0.054 $MgCl_2$	6.19×10^{-3}		γ-FeOOH
17	Ca	1×10^{-3}	Zn	3×10^{-6}–7.6×10^{-7}	0.01 $NaNO_3$	1.8×10^{-4}		$Fe(OH)_3$(am)

[a] For Cd alone $pH_{50\%} = 6.7$. [b] This study.

Table III. Surface Acid/Base and Electrolyte Sorption Reactions and Aqueous Speciation Reactions with Associated Equilibrium Constants

reaction	log K_r TLM	log K_r NEM
$XOH + H^+ \leftrightarrow XOH_2^+$	5.4[a]	4.7[b]
$XOH \leftrightarrow XO^- + H^+$	−10.4[a]	−10.3[b]
$XOH + H^+ + NO_3^- \leftrightarrow XOH_2^+\text{-}NO_3^-$	7.5[a]	6.3[b]
$XOH + Na^+ \leftrightarrow XO^-\text{-}Na^+ + H^+$	−8.3[a]	−9.1[b]
$H_2O \leftrightarrow H^+ + OH^-$	−14.0[c]	−14.0[c]
$Cd^{2+} + H_2O \leftrightarrow CdOH^+ + H^+$	−10.08[c]	=10.08[c]
$Cd^{2+} + 2H_2O \leftrightarrow Cd(OH)_2^0 + 2H^+$	−20.35[c]	−20.35[c]
$Cd^{2+} + 3H_2O \leftrightarrow Cd(OH)_3^- + 3H^+$	−33.30[c]	−33.30[c]
$Cd^{2+} + 4H_2O \leftrightarrow Cd(OH)_4^{2-}$	−47.35[c]	−47.35[c]
$2Cd^{2+} + H_2O \leftrightarrow Cd_2(OH)^{3+} + H^+$	−9.39[c]	−9.39[c]
$Cd^{2+} + NO_3^- \leftrightarrow CdNO_3^+$	0.399[c]	0.399[c]
$Ca^{2+} + H_2O \leftrightarrow CaOH^+ + H^+$	−12.60[c]	−12.60[c]
$Ba^{2+} + H_2O \leftrightarrow BaOH^+ + H^+$	−13.36[c]	
$Sr^{2+} + H_2O \leftrightarrow SrOH^+ + H^+$	−13.18[c]	
$Mg^{2+} + H_2O \leftrightarrow MgOH^+ + H^+$	−11.79[c]	

[a] Davis and Leckie (*1*). [b] Fit to potentiometric titration data in Davis (*27*). [c] Ball et al. (*28*).

as that of the TLM. The solution reactions and associated complexation constants used in this model are also given in Table III. This model has been discussed in greater detail by Krupka et al. (*29*).

The standard deviations for the adsorption constants were estimated by FITEQL by assuming 1% relative and 5% absolute error in the experimental data.

Results and Discussion

Single-Element Adsorption. Cadmium. The fractional adsorption of Cd (10^{-6} and 10^{-7} M) increased from 0 to 100% over the pH range from 5 to 8.5 (Figure 1) and was identical with that noted by other investigators (*13*, *14*, *30*, *31*). The pH of 50% adsorption was 6.4 for 10^{-7} M Cd and 6.7 for 10^{-6} M Cd. As is typical of cation adsorption, the pH of 50% adsorption increased as the concentration of the cadmium and thus the ratio of adsorbate (Cd) to adsorbent [$Fe_2O_3 \cdot H_2O$(am)] increased (*13*, *14*).

Individual Alkaline-Earth Elements. Because Ca^{2+} is a dominent electrolyte ion in soil solutions and groundwater, its adsorption behavior on $Fe_2O_3 \cdot H_2O$(am) was investigated over ranges of concentration and electrolyte ion concentration (Figure 2) representative of typical environmental conditions. The adsorption of Ca, like that of Cd, increased with pH, consistent with the observations of other researchers (*17*, *32*, *33*). The effect of pH was most marked for the lowest Ca concentrations (curve a in Figure 2). The adsorption of Ca was shifted to a higher pH than that of Cd, which was a result of both the higher concentration of Ca (and therefore higher adsorbate-to-adsorbent ratio) and its lower affinity for the surface. With constant initial Ca concentration, increasing the ionic strength through $NaNO_3$ addition decreased Ca adsorption (curves b, d, and e in Figure 2).

The decrease in Ca adsorption with increasing initial solution concentration could have been caused by a shortage of ionized sites available to complex with the Ca. As illustrated in Table IV, the amount of Ca sorbed on the surface of the $Fe_2O_3 \cdot H_2O$(am) at pH 10 increased less than 1 order of magnitude when the initial concentration of Ca increased almost 2 orders of nagnitude or the ionic strength increased 2 orders of magnitude. As the concentration of Ca in solution increased relative to the $Fe_2O_3 \cdot H_2O$(am) concentration (i.e., Ca/Fe molar ratio increased), the calculated percentages of the ionized and total sites occupied by sorbed Ca increased. However, the increase in percentage of sites occupied was not proportional to the increase in Ca concentration.

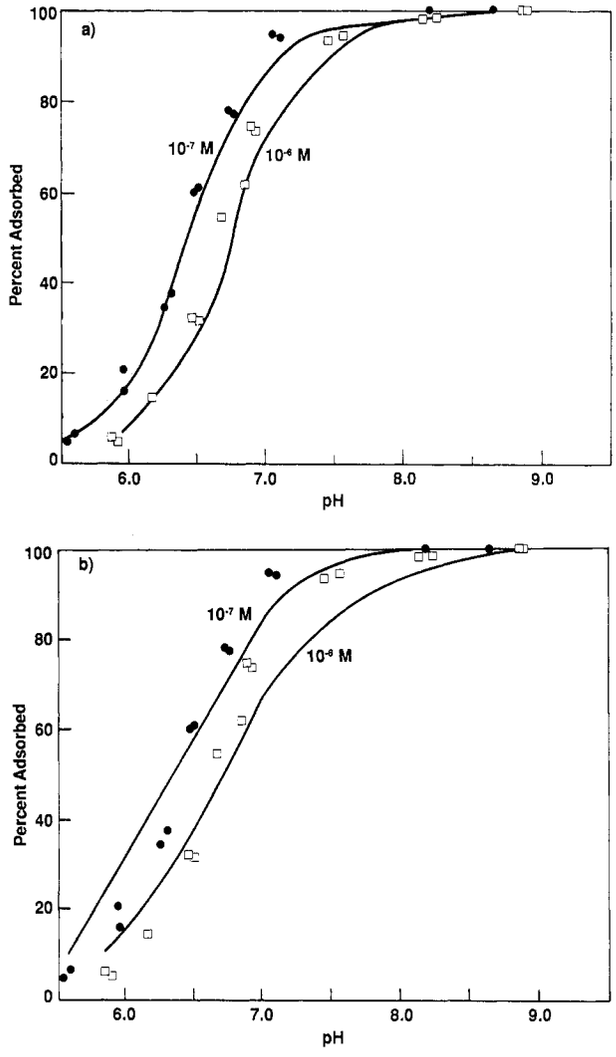

Figure 1. Adsorption of 10^{-7} and 10^{-6} M Cd onto amorphous iron oxyhydroxide (0.87 mM Fe) at I = 0.1 M. (a) Experimental data and predicted sorption using inner-sphere representation of sorption reaction and triple-layer model. (b) Experimental data and predicted sorption using nonelectrostatic model representation of sorption reaction.

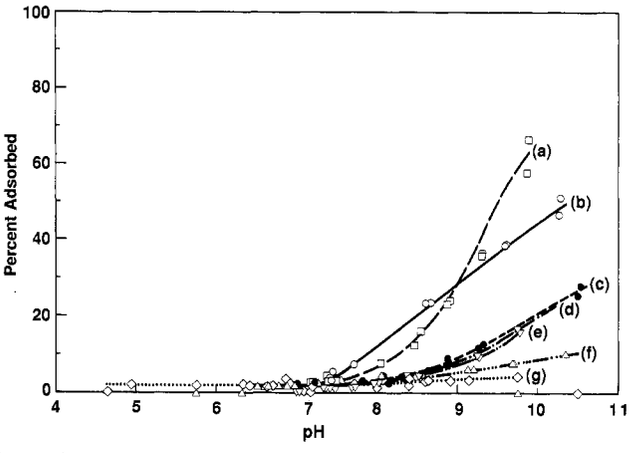

Figure 2. Adsorption of Ca onto amorphous iron oxyhydroxide. (a) [Ca] = 0.027 mM, I = 0.1 M, 0.79 mM Fe. (b) [Ca] = 0.1 mM, I = 0.005 M, 0.77 mM Fe. (c) [Ca] = 0.202 mM, I = 0.1 M, 0.79 mM Fe. (d) [Ca] = 0.1 mM, I = 0.1 M, 0.78 mM Fe. (e) [Ca] = 0.1 mM, I = 0.5 M, 0.78 mM Fe. (f) [Ca] = 0.764 mM, I = 0.1 M, 0.87 mM Fe. (g) [Ca] = 2.4 mM, I = 0.1 M, 0.81 mM Fe.

Table IV. Experimental Conditions for Calcium Adsorption onto Amorphous Iron Oxyhydroxide

Ca concn, M	ionic strength, M $NaNO_3$	iron oxide concn, mM	amt sorbed,[a] M	total surface sites occupied, %	ionized sites occupied,[b]	ref
0.027×10^{-3}	0.1	0.79	1.85×10^{-5}	3.8	40	*c*
0.202×10^{-3}	0.1	0.79	4.06×10^{-5}	8.4	66	*c*
0.764×10^{-3}	0.1	0.87	6.77×10^{-5}	12.5	66	*c*
2.40×10^{-3}	0.1	0.81	1.11×10^{-4}	22.4	71	*c*
1.0×10^{-4}	0.005	0.77	4.38×101^{-5}	9.3	80	*c*
1.0×10^{-4}	0.1	0.78	1.95×10^{-5}	4.1	41	*c*
1.0×10^{-4}	0.5	0.78	1.99×101^{-5}	4.2	23	*c*
1×10^{-4}	0.01	9.55	9.00×10^{-5}	4.1		17
2×10^{-4}	0.01	3.55	1.20×10^{-4}	5.5		17
1×10^{-3}	1	93	1.00×10^{-3}	1.8		33

[a] Amount sorbed at pH 10. [b] Total ionized sites calculated as the sum of XO^-, XO^-–Na^+, and sites occupied by adsorbed Ca. [c] This study.

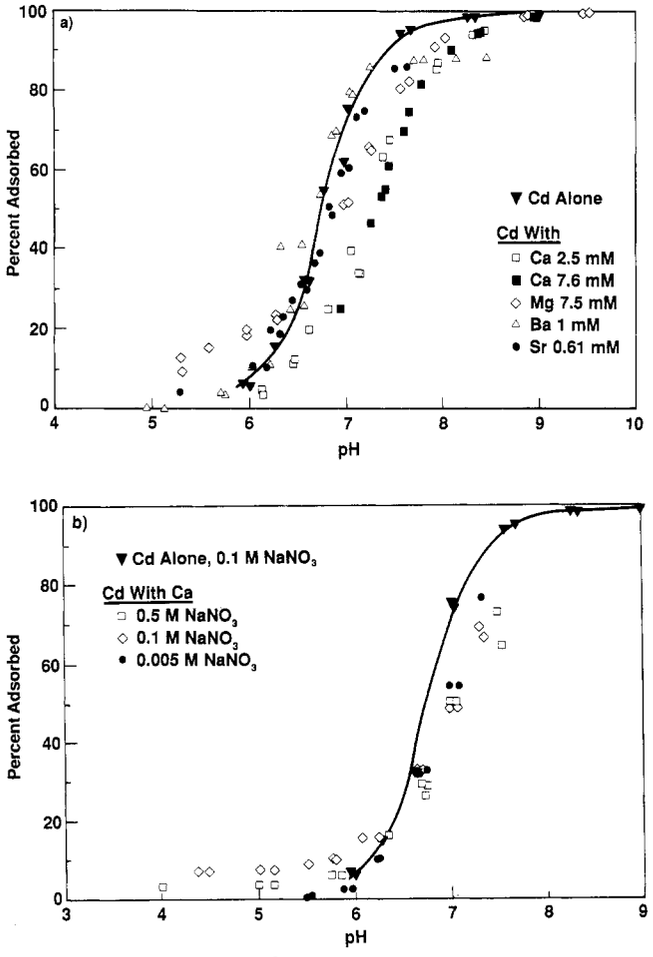

Figure 3. Adsorption of (10^{-6} M) Cd on amorphous iron oxyhydroxide in the presence of alkaline-earth elements. (a) For elements at concentrations given with 0.87 mM Fe in 0.1 M $NaNO_3$. (b) For 2.5 mM Ca with 0.80 mM Fe at ionic strengths given.

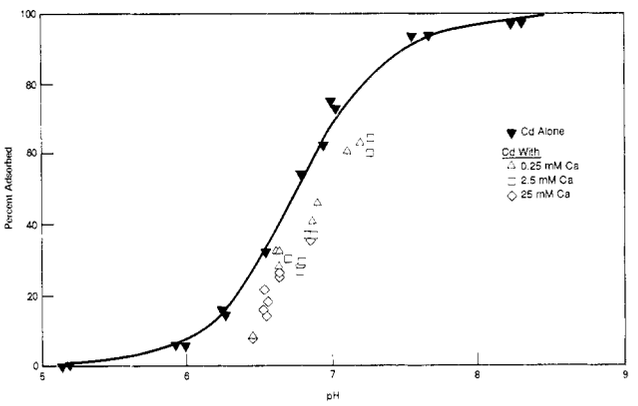

Figure 4. Desorption of adsorbed (10^{-6} M) Cd from amorphous iron oxyhydroxide (0.87 mM Fe) by Ca addition at concentrations given in 0.1 M $NaNO_3$.

Binary-Element Adsorption. The binary-element adsorption edges show Cd competition with Ca and, to a lesser extent, with Mg (Figure 3a). The concentrations of alkaline-earth elements were chosen to be less than the concentration at which either hydroxide or carbonate solids could form; thus, the solution concentrations of Sr and Ba were limited to values lower than could be used for Ca or Mg. Increasing the ionic strength (by means of $NaNO_3$ addition) over 2 orders of magnitude at constant Ca (2.5 mM) and Cd (10^{-6} M) concentrations had minimal effect on the competition (Figure 3b), especially over the pH range 6–7.5. This finding parallels the observation that, in the absence of Ca, Cd adsorption is insensitive to ionic strength (Na concentration) (*20*). The pH of 50% adsorption for each of these experiments, along with published data from other similar binary-element adsorption studies on iron oxides, are given in Table II.

The addition of Ca (at 0.25, 2.5, and 25 mM) was found to desorb Cd from $Fe_2O_3 \cdot H_2O$(am) (Figure 4). The addition of Ca at all concentrations resulted in decreased adsorption of Cd, as was observed for the Cd–Ca competition experiments where the $Fe_2O_3 \cdot H_2O$(am) was loaded with the Ca first (Figure 3a,b). Desorption data at 4, 24, 48, and 144 h (not shown) indicated that equilibrium was achieved rapidly, given that the fractional Cd adsorption after 24 h in the desorption experiment with 2.5 mM Ca was equal to that in the sorption experiment in which Ca was added first. Thus, it appears that the competitive effects were not dependent on the order of loading and were reversible. These results also showed that, above a certain Ca concentration, addition of Ca did not result in further desorption because Cd adsorption in the presence of 2.5 and 25 mM of Ca was equal.

Overall, these results suggest that competition between Cd and Ca is limited to a fixed portion of mutually accessible surface sites. We observed competition when Ca occupied 66% or more of the ionized sites and more than 8% of the total surface sites (Table II). Competition decreased as the Ca concentration and the site coverage by Ca decreased. These conclusions based on coverage of ionized sites are consistent with Dzombak's finding (*34*) that competitive effects are only important when full site coverage is approached. The lack of competition between Cd and Ba or Sr could not be accounted for by differences in site coverage, because even at site coverages where competition between Cd and Ca was observed, no competition with Ba and Sr was observed. Thus, site coverage alone did not explain the presence or absence of competitive sorption between Cd and the different alkaline-earth

elements. The lack of effect of Sr and Ba on Cd adsorption is probably due to these two elements being less strongly sorbed to amorphous iron oxyhydroxide than Ca.

Absorption Modeling. Several surface-complexation models have been used to describe sorption phenomena in a variety of environmental contexts (*3*, *35–37*). These surface-complexation models differ in the number of planes within the solid–liquid interface in which ion adsorption is assumed to occur, and in how and to what extent electrostatics are propagated through this interface (i.e., double layer). These models include (1) the triple-layer model (*1*, *20*), (2) the constant-capacitance model (*19*, *38*), (3) the diffuse-layer model (*34*), and (4) the nonelectrostatic model (*19*, *29*). Many of these models have been shown to provide equivalent representations of metal ion adsorption on oxides (*18*), but their ability to accurately describe competitive sorption phenomena in natural waters has not been addressed. For this reason, the most complex (TLM) and the least complex (NEM) of the site-binding models, where "complex" is used to indicate the number of adjustable parameters, were evaluated for their ability to describe the binary Ca–Cd sorption data.

The surface complexes used in the subsequent analyses are hypothetical and were chosen for their ability to represent the adsorption data. The conclusion that surface complexes similar to those used in the present modeling analyses do form has been supported by spectroscopy (*9*, *39*). However, the fact that the different surface complexes can represent the adsorption data is not proof that these complexes actually exist on the sorbate surface.

Cadmium Adsorption. The Cd data were modeled in two ways by use of the TLM. In the first, Cd was assumed to form only inner-sphere complexes (i.e., complexes in the o-plane). The inner-sphere surface complex represents a close approach to the surface by the element and a strong chemical interaction between the element and the surface, and this behavior is one possible explanation for the observation that Cd sorption is insensitive to the ionic strength of the supporting electrolyte solution (*20*). The formation of such complexes has been hypothesized for strongly adsorbed cations, such as Cu, Pb, Ni, and Cd (*20*). The inner-sphere surface complexation reaction was represented by

$$Cd^{2+} + XOH \leftrightarrow XOCd^{+} + H^{+} \quad (1)$$

where XOH represents a surface site. The fitted log K value for this reaction was -1.9 ± 0.05 for 10^{-6} M Cd and -1.4 ± 0.04 for 10^{-7} M Cd. Only the single inner-sphere surface complex with Cd was required to represent the data for Cd adsorption on $Fe_2O_3 \cdot H_2O$(am) at $I = 0.1$ M (Figure 1a). Hayes and Leckie (*20*) also found that only this single complex was required to model the adsorption of Cd and Pb on goethite.

In the second TLM modeling approach, Cd was assumed to form only outer-sphere complexes (i.e., complexes in the β-plane). This approach was consistent with past modeling of metal ion adsorption (*1*, *5*, *13*, *14*, *30*). The surface-complexation reactions were represented by

$$Cd^{2+} + XOH \leftrightarrow XO^{-}\text{–}Cd^{2+} + H^{+} \quad (2)$$

and

$$Cd^{2+} + XOH + H_2O \leftrightarrow XO^{-}\text{–}CdOH^{+} + 2H^{+} \quad (3)$$

The fitted sorption constants were -9.3 ± 0.04 and -10.7 ± 0.04 for the two reactions for 10^{-6} M Cd at $I = 0.1$ M and -9.3 ± 0.04 and -10.4 ± 0.04 for the two reactions for 10^{-7} M Cd at $I = 0.1$ M. It was necessary to include surface species containing both Cd^{2+} and $CdOH^{+}$ to describe the sorption of Cd when outer-sphere surface complexes were assumed. The fit to the data was slightly better for the inner-sphere surface complex than for the outer-sphere surface complexes.

For the NEM, cadmium was assumed to form only one surface complex. The surface complexation reaction was

$$Cd^{2+} + XOH \leftrightarrow XOCd^{+} + H^{+} \quad (4)$$

The fitted sorption constants were -3.1 ± 0.04 and -2.8 ± 0.04 for 10^{-6} and 10^{-7} M Cd, respectively, at $I = 0.1$ M. The NEM fit to the Cd adsorption edge data was not quite as good as that of the TLM. The Cd adsorption edge calculated by the NEM was flatter (rose less steeply) than the measured adsorption edge (Figure 1b). The applicability of the NEM to a larger range in Cd^{2+} and $Fe_2O_3 \cdot H_2O$(am) concentrations was shown by Krupka et al. (*29*).

For all three representations, the adsorption constants for the two initial Cd concentrations at $I = 0.1$ M were statistically different. The 10^{-7} M Cd constants indicate greater affinity of the Cd for the surface than do the 10^{-6} M Cd constants. This observation is consistent with what would be expected with a heterogeneous surface where the average site energy, and thus the average sorption constant, decreases with increasing site coverage.

Calcium Adsorption. Several types of surface-complexation reactions were evaluated by using both the TLM and the NEM for describing the calcium adsorption data. The TLM reactions included various outer-sphere complexes and a combination of both inner- and outer-sphere complexes. The combination of inner- and outer-sphere complexes was found to be necessary to model the binary Cd–Ca experiments.

Most of the surface complexes evaluated for Ca were outer-sphere surface complexes consistent with most past modeling. Outer-sphere complex formation represents a weak complex with the surface and may account for the sensitivity of Ca and other alkaline-earth element sorption to ionic strength (Figure 2; refs 20, 32, and 40). The outer-sphere surface complexation reactions evaluated included (1) complexes with Ca^{2+} and $CaOH^{+}$, both individually and together, and (2) the bidentate complex with Ca^{2+}, both individually and together with $CaOH^{+}$. Dempsey and Singer (*17*) and Balistrieri and Murray (*41*) used the bidentate complex to represent the sorption of alkaline-earth elements on $Fe_2O_3 \cdot H_2O$(am) and goethite, respectively. In this study, the two outer-sphere surface complexation reactions that best represented the data for the TLM were the bidentate complex with Ca^{2+}

$$Ca^{2+} + 2XOH \leftrightarrow (XO^{-})_2\text{–}Ca^{2+} + 2H^{+} \quad (5)$$

and the complex with $CaOH^{+}$

$$Ca^{2+} + XOH + H_2O \leftrightarrow XO^{-}\text{–}CaOH^{+} + 2H^{+} \quad (6)$$

The fitted constants for these two reactions are given in columns 6 and 7 of Table V. For comparison, the fitted constants for the outer-sphere complexes with Ca^{2+} and $CaOH^{+}$ are given in columns 4 and 5 of Table V. Our constants for the outer-sphere complexes with Ca^{2+} and $CaOH^{+}$ were very similar to those determined by Balistrieri and Murray (*3*) for Ca in seawater (log $*K$ is -5.0 for Ca^{2+} and -14.5 for $CaOH^{+}$ at $I = \sim 0.7$ M).

To accurately model the observed competition between Ca and Cd, Ca was hypothesized to form a combination of inner- and outer-sphere complexes. The inner- and outer-sphere complexes that best represented the single-element sorption data were

$$Ca^{2+} + 2XOH \leftrightarrow (XO^{-})_2\text{–}Ca^{2+} + 2H^{+} \quad (7)$$

for the outer-sphere complex and

$$Ca^{2+} + XOH \leftrightarrow XOCa^{+} + H^{+} \quad (8)$$

Table V. Fitted Surface Sorption Constants for Calcium on Amorphous Iron Oxyhydroxide

			triple-layer model						
			outer sphere		outer sphere		inner and outer sphere		
Ca, mM	Fe, mM	ionic strength, M $NaNO_3$	log *K XO–Ca^{2+} [a]	log *K XO–$CaOH^+$ [b]	log *K XO–$CaOH^+$ [b]	log *K bidentate[c]	log *K outer[c]	log *K inner[d]	NEM[e] log K[d]
2.4	0.81	0.1	−1.55 ± 1.5	−14.3 ± 1.7	−14.2 ± 1.7	−7.52 ± 1.3	−7.55 ± 1.3	−7.87 ± 4.0	−7.15 ± 0.49
0.764	0.87	0.1	−4.45 ± 0.65	−15.3 ± 0.37	−15.3 ± 0.37	−10.0 ± 0.46	−10.0 ± 0.45	−8.36 ± 0.73	−6.80 ± 0.14
0.202	0.79	0.1	−4.43 ± 0.37	−14.9 ± 0.19	−14.9 ± 0.18	−9.62 ± 0.26	−9.60 ± 0.25	−8.48 ± 0.31	−6.42 ± 0.08
0.027	0.79	0.1	−5.03 ± 0.21	−14.0 ± 0.08	−14.0 ± 0.09	−9.74 ± 0.15	−9.66 ± 0.13	−6.97 ± 0.17	−5.64 ± 0.04
0.1	0.77	0.5	−5.43 ± 0.59	−14.5 ± 0.15	−14.5 ± 0.16	−10.1 ± 0.40	−10.0 ± 0.37	−7.36 ± 0.34	−6.17 ± 0.10
0.1	0.78	0.1	−4.92 ± 0.35	−15.4 ± 0.15	−15.4 ± 0.20	−9.86 ± 0.23	−9.85 ± 0.23	−9.21 ± 0.46	−6.52 ± 0.06
0.1	0.78	0.005	−3.47 ± 0.47	−14.1 ± 0.15	−14.1 ± 0.14	−8.38 ± 0.34	−8.25 ± 0.31	−8.17 ± 0.23	−6.30 ± 0.05
combined 0.1 mM Ca data			−4.87 ± 0.22	−15.0 ± 0.09	−15.0 ± 0.09	−9.77 ± 0.14	−9.72 ± 0.13	−8.46 ± 0.17	−6.38 ± 0.04

[a] $Ca^{2+} + XOH \leftrightarrow XO^-–Ca^{2+} + H^+$. [b] $Ca^{2+} + H_2O + XOH \leftrightarrow XO^-–CaOH^+ + 2H^+$. [c] $Ca^{2+} + 2XOH \leftrightarrow (XO^-)_2–Ca^{2+} + 2H^+$. [d] $Ca^{2+} + XOH \leftrightarrow XOCa^+ + H^+$. [e] Nonelectrostatic model.

for the inner-sphere complex. The adsorption constants for each set of data are presented in columns 8 and 9 of Table V.

For the NEM, only one complexation reaction

$$Ca^{2+} + XOH \leftrightarrow XOCa^+ + H^+ \quad (9)$$

was required to represent the sorption of Ca on the $Fe_2O_3·H_2O$(am) (column 10 of Table V).

The TLM and NEM surface-complexation constants for different initial Ca concentrations and ionic strengths varied by as much as 1 log unit and thus were neither constant nor "intrinsic" [as described by Sposito (*9*) and Westall and Hohl (*18*)]. Previous researchers have suggested that this variation in adsorption constants is related to surface coverage and reflects the heterogeneity of the surface, which causes the metal ion to be adsorbed to less and less energetic sites as the surface coverage increases (*42*). That surface sites and their affinities vary would appear to be reasonable for crystalline oxides such as goethite, because different crystal faces with different surface energies and site characteristics (*9*) are exposed and because the crystalline surfaces have pits, edges, and other discontinuities as a result of surface defects (*42*). In fact, Vanek and Jedinakova (*43*), who investigated the sorption of Ba on goethite (α-FeOOH) over a range in Fe/Ba ratios, observed that the strength of sorption of Ba varied with surface coverage. However, amorphous solids such as $Fe_2O_3·H_2O$(am) appear to be characterized by a larger number of low-affinity sites (*44*) and a small number of high-affinity sites (*45*). Linear regression analysis (*46*) of the log *K values for the various surface complexes indicated that neither surface coverage, initial Ca concentration, nor ionic strength, whether alone or in combination, could explained the observed variability.

These results illustrate the fact that single-element models that assume a single binding energy (i.e., conformation to a Langmuir isotherm) cannot adequately describe sorption over a range in surface coverage for sorbate–sorbent pairs that conform to a Freundlich isotherm as a result of site heterogeneity rather than electrostatic effects (*47*). Even though the experimental data suggested that the surface was heterogeneous with regard to Ca adsorption, a single-site model was used to model the individual Ca and Cd adsorption data and the combined Cd–Ca adsorption data. Although it is possible that concentration-independent Ca adsorption constants could be derived by using a multisite model, the single-site model was used because there is no consensus on how best to represent surface heterogeneity or on how this heterogeneity affects competition. The multisite model has been used by Dzombak and Morel (*48*, *49*), to successfully model cation sorption on oxides.

Binary-Element Adsorption. To evaluate the effectiveness of the TLM and NEM in predicting the measured competition, the binary-element experiments with Cd and Ca were modeled using different hypothesized surface reactions and combinations of surface reactions. For each representation of the surface reactions, the 2.4 mM Ca constants in Table V for 0.1 M $NaNO_3$ were used to calculate the effects of Ca adsorption, because the Ca concentration in the competition experiments (2.5 mM) was close to this value. The range in Ca constants in Table V for each surface reaction was used to evaluate the sensitivity of the predicted Cd sorption to this variability. For each representation of the surface reactions, the Cd adsorption constants for 10^{-6} M Cd at I = 0.1 M were used to calculate the Cd adsorption.

Regardless of which set of Ca adsorption constants was used to represent the Ca adsorption, when the inner-sphere complex for Cd adsorption was used in combination with only outer-sphere complexes for Ca (columns 6 and 7 of Table V), no competition was calculated and the adsorption curve predicted was identical with that for cadmium adsorption alone (Figure 5). Variation of the Ca outer-sphere adsorption constants within the range noted in Table V resulted in no more than a 1% difference between the predicted Cd sorption and that shown in Figure 5. The lack of competition between Cd and Ca and the insensitivity of Cd adsorption to variation in the Ca constants were not unexpected because, within the model, these two elements were placed in different planes with respect to the surface. Adsorbed Ca, because of its location in the more remote β-plane, cannot induce a mass-action effect on Cd in the surface or o-plane. The calculated effects are solely electrostatic and therefore minimal.

Use of outer-sphere complexes for both Cd and Cd (columns 6 and 7 of Table V) resulted in prediction of more competition than was observed (Figure 5). The Cd adsorption was very sensitive to variation in the Ca constants. In fact, when the 0.764 mM Ca constant was used to represent Ca adsorption, the predicted Cd adsorption was close to the measured sorption. The similarity in shape of the observed and predicted adsorption edges when outer-sphere complexes are used for both Cd and Ca suggests that this representation in the TLM was more accurate than the previous TLM representation. The fact that the competition data were better represented when the outer-sphere complexes were assumed for both Cd and Ca would be consistent with competition being driven by mass action rather than electrostatic effects. In other

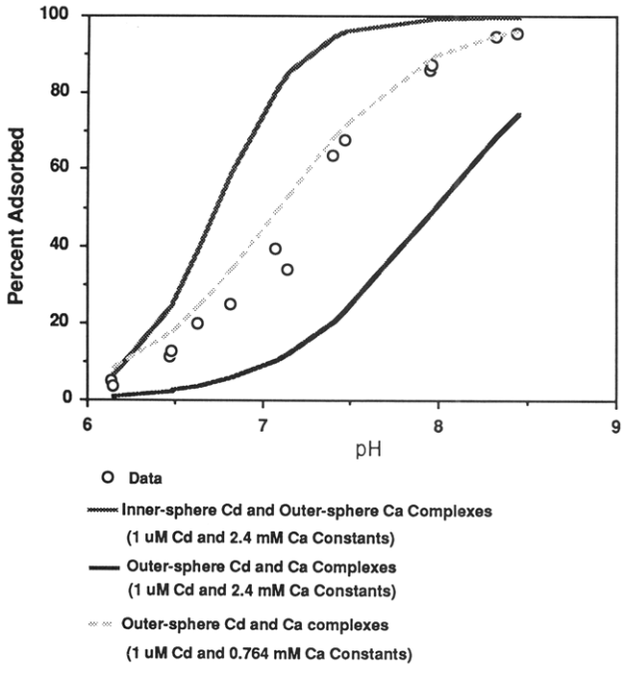

Figure 5. Comparison of experimental data for Cd adsorption in the presence of Ca with that predicted by TLM using various combinations of surface reactions. Experimental conditions are 10^{-6} M Cd and 2.5 mM Ca with 0.87 mM Fe in 0.1 M $NaNO_3$.

modeling studies where the competing ions have been assumed to occupy the same plane to to compete for the same surface sites, the amount of competition predicted was also excessive (*14*, *42*, *50*).

The previous TLM calculations indicated that the competitive effect of Ca on Cd cannot be reproduced unless at least some of the Ca is allowed to adsorb within the same plane as Cd and thus to compete by means of mass action. In an attempt to derive a TLM that better represented the competition data, it was hypothesized that the Ca formed a combination of inner- and outer-sphere complexes and Cd formed only an inner-sphere complex. In this representation, the inner-sphere Ca and Cd complexes would account for the mass-action competition between the Cd and Ca on mutually accessible sites and the outer-sphere Ca complex would account for the additional Ca sorption and the variation in Ca adsorption with ionic strength.

The Cd adsorption predicted in the Ca–Ca experiments using the inner-sphere complex for Cd and a combination of inner- and outer-sphere complexes for Ca in the TLM (columns 8 and 9 of Table V) was in good agreement with the experimental data at I = 0.5 M (Figure 6a) and I = 0.1 M (Figure 6b) but deviated from the experimental results at the lowest ionic strength, I = 0.005 M (Figure 6c). For all three ionic strengths, the sorption edge predicted by the TLM was steeper than the measured sorption edge. In contrast to the other TLM representations, when the Ca adsorption constants were varied over the range shown in Table V, the predicted Cd adsorption did not differ by more than 2% from that shown in Figure 6.

Like the previous TLM representation, the NEM model also provided predictions of Cd (10^{-6} M) adsorption in the presence of Ca (2.5 mM) that were close to the experimental results for the two highest ionic strengths (Figure 7a,b) and less satisfactory at the lowest ionic strength (Figure 7c). When the NEM adsorption constant for Ca was varied over the range given in Table V, the predicted Cd adsorption did not differ from that shown in Figure 7 by more than 1%. The very close agreement between the observed and predicted Cd adsorption at the two

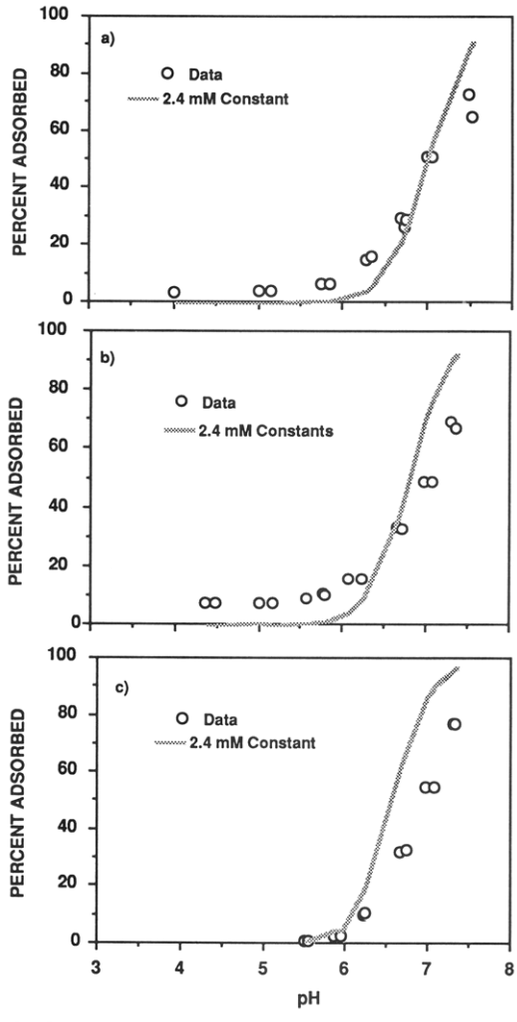

Figure 6. Comparison of experimental data for Cd adsorption in the presence of Ca with that predicted by TLM using inner- and outer-sphere adsorption constants for Ca and inner-sphere adsorption constant for Cd. Experimental conditions are 10^{-6} M Cd and 2.5 mM Ca with 0.87 mM Fe. (a) I = 0.5 M. (b) I = 0.1 M. (c) I = 0.005 M.

highest ionic strengths (Figure 7a,b), while not substantially better than that with the TLM, had special meaning because this model is simple, employing only one surface complex for Ca, one for Cd, and no electrostatics. The NEM calculations showed that the Cd–Ca competition was consistent with a mass-action effect between the Ca and Cd on mutually accessible surface sites. The shape of the Cd–Ca sorption edges predicted from the NEM (Figure 7a–c) was much closer to that of the measured Cd–Ca adsorption edge than the Cd–Ca adsorption edges predicted by using the TLM were (Figure 6a–c).

These modeling results imply that the Cd–Ca competition is due to a mass-action effect between the Cd and Ca, and that electrostatics are of little importance. Additionally, the lack of appreciable ionic strength effect on the Cd–Ca competition (Figure 3b) suggests that Na is not a significant competitor for the sites that are mutually accessible to Cd and Ca. The electrostatic component of the TLM makes the predicted adsorption edge rise more rapidly with pH than was observed. Electrostatic effects on the adsorption of cations should be important only when the surface becomes saturated with the cations and the surface charge is reversed (*34*).

Implications of Binary-Element Modeling. Surface-complexation models have been used with varying success to predict multielement sorption using adsorption constants calculated from single-element adsorption ex-

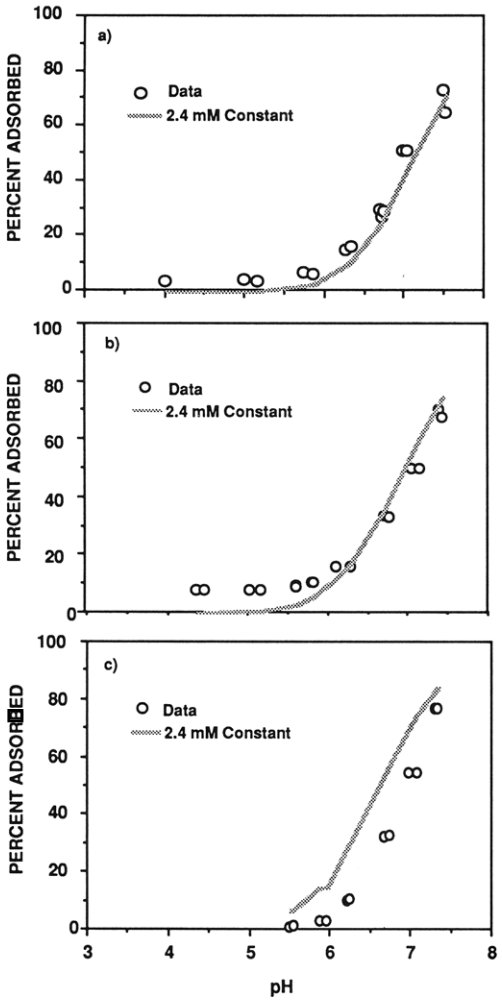

Figure 7. Comparison of experimental data for Cd adsorption in presence of Ca with that predicted by NEM. Experimental conditions are 10^{-6} M Cd and 2.5 mM Ca with 0.87 mM Fe. (a) I = 0.5 M. (b) I = 0.1 M. (c) I = 0.005 M.

periments. Single-element adsorption constants have been used to qualitatively predict the adsorption of CrO_4^{2-} in the presence of SO_4^{2-} and dissolved inorganic carbon on $Fe_2O_3 \cdot H_2O$(am) (*22*) and oxide-containing subsurface soils (*23*). Also, Balistrieri and Murray (*3*) modeled the competitive effect of Mg on Cd adsorption onto goethite in artificial seawater using this approach. Their modeling results were consistent with the results shown here, in that the best approximation to the competition data using the TLM was found for high ionic strengths (I = 0.5 M), when inner-sphere complexes for Mg and Cd would predominate (e.g., Figure 6a). In contrast, Goldberg and Traina (*50*) found that constant-capacitance surface-complexation constants fit to the single-element sorption data predicted too much competition between the strongly sorbing anion orthophosphate and the anions selenite and silicate on goethite. Benjamin (*42*) found that single-element sorption constants representing outer-sphere complexes resulted in overprediction of the competitive sorption of Cd in the presence of Cu, Zn, and Pb on $Fe_2O_3 \cdot H_2O$(am).

Goldberg and Traina (*50*) argued that it was not possible to closely predict binary-element sorption data from single-element sorption constants because of either site heterogeneity or incorrect estimates of the activity coefficient of the surface complexes. Site heterogeneity could cause some of the sites to selectively adsorb one element over the other. Furthermore, as a result of competition, an element could become sorbed to less energetic sites than were encountered in the single-element sorption. Because the electrostatic term in the TLM can be considered as the sorbed-phase activity coefficient corrected for the charge of the sorbed species (*9*), an inaccurate representation of this term could make it impossible to accurately predict the degree of competition. Other factors not explicitly accounted for by the electrostatic term may also influence the sorbate surface's activity coefficients. Chu and Sposito (*51*) argued that, for this reason, binary exchange data are not sufficient to model ternary exchange and that some information on the ternary exchange is necessary to accurately estimate the activity coefficients. However, their example indicated that these additional data are not always required.

To avoid the problem of how to represent surface heterogeneity and surface activity coefficients, Goldberg and Traina (*50*) recommended that constants be fitted for each of the two elements by using the competition data. This approach is reasonable if the objectives of the model are to predict competition for similar experimental conditions. The new constants would have limited value for predicting competition for other solution compositions. For example, these constants would not accurately predict the single-element sorption data. Furthermore, this approach would require that constant be derived for every solution composition of interest. If the objective of the modeling is, instead, to develop an approach for predicting multielement adsorption from basic data such as that describing the adsorption of the single elements, then another approach must be developed.

The ability of the TLM with a combination of inner- and outer-sphere surface complexes and the NEM to predict the Cd–Ca competition at the highest ionic strengths implies that a credible modeling approach using single-element adsorption constants could be developed. These two models are not overly sensitive to variations in the adsorption constants of the single elements, suggesting that such a model could also be quite stable. In addition, the fact that both the TLM and NEM were able to predict the competition at the highest ionic strengths with a set of constants fit to the single-element sorption data suggests that, at ionic strengths greather than 0.1 M, the Cd adsorption is not shifted to lower energy sites by competition with Ca. Finally, these results suggest that surface heterogeneity may not be an important factor when the ionic strength is approximately 0.1 M or more. However, it is possible that site heterogeneity on $Fe_2O_3 \cdot H_2O$(am) could account for both models' inability to predict the Cd–Ca competition in the lowest ionic strength solution.

Conclusions

The binary-element experiments indicate that, at typical environmental concentrations, the alkaline-earth elements Mg, Sr, and Ba will have little effect on the adsorption of Cd and similar elements on $Fe_2O_3 \cdot H_2O$(am). Solubility limitations in soil and groundwater systems will prevent Sr and Ba from reaching concentrations high enough to allow them to compete with Cd on iron oxides. However, competitive adsorption of Cd with Ca can be important in soil or groundwater. Competition between Cd and Ca was observed over ranges of Ca concentrations and pH that are environmentally important. When competition occurs, the percentage of Cd adsorbed could fall by 20% or more below that for Cd alone, depending on the pH and on the concentrations of Cd and Ca in the soil solutions, groundwater, or leachate.

Application of electrostatic (TLM) and nonelectrostatic (NEM) surface-complexation models showed that the competitive effect was consistent with a mass-action effect

between Ca and Cd on mutually accessible surface sites. The TLM accurately represented the results of the competition experiments in the high (I = 0.5 M) and medium (I = 0.1 M) ionic strength solutions only when a combination of inner- and outer-sphere surface complexes for Ca and an inner-sphere complex for Cd were included in the model. The NEM, which includes only one adsorption plane, one surface complex each for Cd and Ca, and no electrostatics, provided predictions of the Cd–Ca competition at high and medium ionic strengths that agreed with the experimental data at least as well as the predictions made by the TLM. Neither model accurately represented the amount of adsorption at the lowest ionic strength (I = 0.005 M), which is the ionic strength most relevant to natural soil solutions or groundwater. No reason for this discrepancy could be identified. Even though the single-element sorption constants of Ca for initial Ca concentrations ranging from 2 orders of magnitude and ionic strengths varying over 3 orders of magnitude differed by as much as 1 log unit, the predicted Cd sorption was not sensitive to this range in the adsorption constants, indicating that both these models were very stable. At all ionic strengths, the NEM simulated the shape of the combined Cd–Ca adsorption edges better than the TLM. These results show that the more complex electrostatic model does not provide calculations of Cd–Ca competition that are improved sufficiently to warrant its application over the nonelectrostatic model. Rather, our evaluation has shown that the NEM using single-element sorption constants can effectively model multielement adsorption for the conditions used in this study. Given the limited range of experimental conditions evaluated, additional investigations are clearly needed to determine whether these two modeling approaches can expediently and accurately predict multielement sorption equilibria under the broad range of solute, contaminant, and electrolyte conditions found in natural waters.

Acknowledgments

Dr. C. Hostetler and Mr. R. Erikson demonstrated to us the usefulness of the NEM for solute adsorption calculations on $Fe_2O_3 \cdot H_2O$(am). In addition, we would like to thank Ms. C. Peyton for performing the initial modeling analyses.

Registry No. Cd, 7440-43-9; Fe_2O_3, 1309-37-1; Ca, 7440-70-2; Mg, 7439-95-4; Sr, 7440-24-6; Ba, 7440-39-3.

Literature Cited

(1) Davis, J. A.; Leckie, J. O. *J. Colloid Interface Sci.* **1978**, *67*, 90–107.
(2) Benjamin, M. M.; Bloom, N. S. In *Adsorption from Aqueous Systems*; Tewari, P. H., Ed.; Plenum: New York, 1981.
(3) Balistrieri, L. S.; Murray, J. W. *Geochim. Cosmochim. Acta* **1982**, *46*, 1253–1265.
(4) Loganathan, P.; Burau, R. G. *Geochim. Cosmochim. Acta* **1973**, *37*, 1277–1293.
(5) Murray, J. W. *Geochim. Cosmochim.* Acta **1975**, *39*, 505–519.
(6) Loganathan, P.; Burau, R. G.; Fuerstenau, D. W. *Soil Sci. Soc. Am. J.* **1977**, *41*, 57–62.
(7) McKenzie, R. M. *Aust. J. Soil Res.* **1980**, *18*, 61–73.
(8) Jenne, E. A. *Adv. Chem. Ser.* **1968**, *No. 73*, 337–387.
(9) Sposito, G. *The Surface Chemistry of Soils*; Oxford University Press: New York, 1984; p 234.
(10) Rai, D.; Zachara, J. M.; Schwab, A. P.; Schmidt, R. L.; Girvin, D. C.; Rogers, J. E. Chemical Attenuation Rates, Coefficients, and Constants in Leachate Migration. EA-3356; prepared for the Electric Power Research Institute; Battelle, Pacific Northwest Laboratories; Richland, WA, 1984.
(11) Sigg, L. In *Aquatic Surface Chemistry*; Stumm, W., Ed.; John Wiley and Sons: New York, 1987.
(12) Kent, D. B.; Tripathi, V. S.; Ball, N. B.; Leckie, J. O. *Surface Complexation Modeling of Radionuclide Adsorption in Subsurface Environments*; NUREG/CR-4897, SAND 86-7175; U.S. Nuclear Regulatory Commission: Washington, DC; 1988.
(13) Benjamin, M. M.; Leckie, J. O. In *Contaminants and Sediments*; Baker, R. A., Ed.; Ann Arbor Science: Ann Arbor, MI, 1980; Vol. 2, Chapter 16.
(14) Benjamin, M. M.; Leckie, J. O. *J. Colloid Interface Sci.* **1981**, *79*, 209–221.
(15) Zasoski, R. J.; Burau, R. G. *Soil Sci. Soc. Am. J.* **1988**, *52*, 81–87.
(16) Swallow, K. C.; Hume, D. N.; Morel, F. M. M. *Environ. Sci. Technol.* **1980**, *14*, 1326–1331.
(17) Dempsey, B. A.; Singer, P. C. In *Contaminants and Sediments*; Baker, R. A., Ed.; Ann Arbor Science: Ann Arbor, MI, 1980.
(18) Westall, J.; Hohl, H. *Adv. Colloid Interface Sci.* **1980**, *12*, 265–294.
(19) Stumm, W.; Hohl, H.; Dalang, F. *Croat. Chem. Acta* **1976**, *43*, 491.
(20) Hayes, K. F.; Leckie, J. O. *J. Colloid Interface Sci.* **1987**, *115*, 564–572.
(21) Balistrieri, L. S.; Murray, J. W. *Am. J. Sci.* **1981**, *281*, 788–806.
(22) Zachara, J. M.; Girvin, D. C.; Schmidt, R. L.; Resch, C. T. *Environ. Sci. Technol.* **1987**, *21*, 589–594.
(23) Zachara, J. M.; Ainsworth, C. C.; Cowan, C. E.; Resch, C. T. *Soil Sci. Soc. Am. J.* **1989**, *53*, 418–428.
(24) Girvin, D. C.; Ames, L. L.; McGarrah, J. E. *J. Colloid Interface Sci.*, in press.
(25) Westall, J. *FITEQL, A Computer Program for Determination of Equilibrium Constants from Experimental Data*; Version 1.2, Report 82-01; Department of Chemistry, Oregon State University: Corvallis, OR, 1982.
(26) Westall, J. *FITEQL, A Computer Program for Determination of Equilibrium Constants from Experimental Data*; Version 2.0, Report 82-02; Department of Chemistry, Oregon State University: Corvallis, OR, 1982.
(27) Davis, J. A. Ph.D. Dissertation, Stanford University, 1978.
(28) Bell, J. W.; Nordstrom, D. K.; Jenne, E. A. *Additional and Revised Thermodynamic Data and Computer Code for WATEQ2—A Computerized Chemical Model for Trace and Major Element Speciation and Mineral Equilibria of Natural Waters*; Water Resources Investigations No. 78-116; U.S. Geological Survey: Menlo Park, CA, 1980.
(29) Krupka, K. M.; Erikson, R. L.; Mattigod, S. V.; Schramke, J. A.; Cowan, C. E.; Eary, L. E.; Morrey, J. R.; Schmidt, R. L.; Zachara, J. M. A Guide to the Thermodynamic Data in the FASTCHEM Package. Prepared for the Electric Power Research Institute; Battelle, Pacific Northwest Laboratories, Richland, WA, 1988.
(30) Benjamin, M. M.; Leckie, J. O. *Environ. Sci. Technol.* **1982**, *16*, 162–170.
(31) Farley, K. J.; Dzombak, D. A.; Morel, F. M. M. *J. Colloid Interface Sci.* **1985**, *106*, 226–242.
(32) Kinniburgh, D. G.; Syers, J. K.; Jackson, M. L. *Soil. Sci. Soc. Am. Proc.* **1975**, *39*, 464–470.
(33) Kinniburgh, D. G.; Jackson, M. L.; Syers, J. K. *Soil Sci. Soc. Am. J.* **1976**, *40*, 796–799.
(34) Dzombak, D. A. Ph.D. Dissertation, Massachusetts Institute of Technology, 1986.
(35) Cederberg, G. A.; Street, R. L.; Leckie, J. O. *Water Resour. Res.* **1985**, *21*, 1095–1104.
(36) Catts, J. G.; Langmuir, D. *Appl. Geochem.* **1986**, *1*, 255–264.
(37) Davis, A.; Runnells, D. D. *Appl. Geochem.* **1987**, *2*, 231–241.
(38) Stumm, W.; Kimmert, R.; Sigg, L. *Croat. Chem. Acta* **1980**, *53*, 291.
(39) Schindler, P. W.; Stumm, W. In *Aquatic Surface Chemistry*; Stumm, W., Ed.; Wiley Interscience: New York, 1987.
(40) Posselt, H. S.; Anderson, F. J.; Weber, W. J., Jr. *Environ. Sci. Technol.* **1968**, *2*, 1087–1093.
(41) Balistrieri, L. S.; Murray, J. W. In *Chemical Modeling in Aqueous Systems*; Jenne, E. A., Ed.; ACS Symposium Series

93; American Chemical Society: Washington, DC, 1979; pp 275-298.
(42) Benjamin, M. M. Ph.D. Dissertation, Stanford University, 1979.
(43) Vanek, K.; Jedinakova, V. *J. Colloid Interface Sci.* **1986**, *111*, 276-279.
(44) Kinniburgh, D. G.; Jackson, M. L. In *Adsorption of Inorganics at Solid-Liquid Interfaces*; Anderson, M. A., Rubin, A. J., Eds.; Ann Arbor Science: Ann Arbor, MI, 1981.
(45) Kinniburgh, D. G.; Baker, J. A.; Whitfield, M. *J. Colloid Interface Sci.* **1983**, *95*, 370-384.
(46) Snedecor, G. W.; Cochran, W. G. *Statistical Methods*, 6th ed.; The Iowa State University Press: Ames, IA, 1976.
(47) Westall, J. C. In *Aquatic Surface Chemistry*; Stumm, W., Ed.; John Wiley and Sons: New York, 1987; Chapter 1.
(48) Dzombak, D. A.; Morel, F. M. M. *J. Colloid. Interface Sci.* **1986**, *112*, 588.
(49) Dzombak, D. A.; Morel, F. M. M. *J. Hydraul. Eng.* **1987**, *113*, 430.
(50) Goldberg, S.; Traina, S. J. *Soil Sci. Soc. Am. J.* **1987**, *51*, 929-932.
(51) Chu, S.-Y.; Sposito, G. *Soil Sci. Soc. Am. J.* **1981**, *45*, 1084-1089.

Received for review January 18, 1989. Revised manuscript received June 18, 1990. Accepted October 10, 1990. This research was funded by the Electric Power Research Institute, Inc. (EPRI) under Contract RP2485-03, Chemical Attenuation Studies, to Battelle, Pacific Northwest Laboratories.

Brominating Activity of the Seaweed *Ascophyllum nodosum*: Impact on the Biosphere

Ron Wever,* Michiel G. M. Tromp, Bea E. Krenn, Abdoeljalal Marjani, and Mauritz Van Tol

E. C. Slater Institute for Biochemical Research and Biotechnological Center, University of Amsterdam, Plantage Muidergracht 12, 1018 TV Amsterdam, the Netherlands

■ Macroalgae are an important source of volatile halogenated organic compounds, such as bromoform and dibromomethane. The mechanism by which these compounds are formed is still elusive. We report that the brown seaweeds *Laminaria saccharina*, *Laminaria digitata*, *Fucus vesiculosis*, *Pelvetia canaliculata*, and *Ascophyllum nodosum* and the red seaweeds *Chondrus crispus* and *Plocamium hamatum* contain bromoperoxidases. The intact plants are able to brominate exogeneous organic compounds when H_2O_2 and Br^- are added to seawater. Further, we show that the brominating activity of the brown macroalga *A. nodosum*, which contains a vanadium bromoperoxidase located on the thallus surface, occurs when the plant is exposed to light and not in the dark. The rate of bromination of exogenous organic compounds in seawater by this plant is 68 nmol (g of wet alga)$^{-1}$ h^{-1}. HOBr is a strong biocidal agent and we propose that the formation of HOBr by this seaweed is part of a host defense system.

Introduction

There is great current interest in the formation of organohalides produced by both anthropogenic activities and biological sources. Recently, it has been suggested (*1*) that chemical reactions occur in the troposphere at polar sunrise in the Arctic. In one of these processes ozone destruction occurs at ground level, which may be connected to the formation of bromoform and aerosol enrichment with bromine of biological origin (*2*). According to Sturges and Barrie (*2*), inorganic bromine in Arctic aerosols may originate from photochemical conversion of marine organic bromine. Measurements (*3*) of atmospheric bromoform at Point Barrow, AK, show that the presence of this compound is seasonal: bromoform concentrations are maximal in winter and minimal in summer. Similarly, the bromine content of Arctic aerosols at Point Barrow, Alert (Canadian Arctic), and Spitsbergen shows an annual sharp maximum between February and May at concentrations that are the highest in the world (*2*, *4*, *5*). There is substantial evidence that the source of the bromine-containing particles and bromoform is biogenic and it has been speculated that the formation is due to the enzymic activity of vanadium bromoperoxidases present in brown seaweeds that grow in the Arctic Ocean (*6*). Indeed, Dyrssen and Fogelqvist (*7*, *8*) showed that bromoform is present in the Arctic Ocean near Spitsbergen and the data clearly indicate that algal belts are responsible for its production. It is well-known that brown seaweeds (*Ascophyllum nodosum*, *Fucus vesiculosis*), red seaweeds (*Gigartina stellata*), and marine green seaweeds (*Enteromorpha linza*, *Ulva lacta*) release large quantities of brominated methanes such as bromoform and dibromomethane into the marine ecosystem (*9*).

Recently, a group of vanadium-containing bromoperoxidases has been discovered in a number of brown seaweeds (*Fucus distichus*, *Alaria esculenta*, *Laminaria saccharina*, *Chorda filum*) and in red seaweeds (*Ceramium rubrum* and *Corallina pilulifera*) (*10-14*). In the presence of hydrogen peroxide and bromide these enzymes (*15*) produce free hypobromous acid and bromine. The peroxidases are assumed to be involved in the biosynthesis of the halogenated metabolites by bromination of nucleophilic acceptors. As has been shown by Theiler et al. (*16*) for the marine red alga *Bonnemaisonia hamifera* and by Burreson et al. (*17*) for the red alga *Asparagopsis taxiformis*, the acceptors are probably carboxy methyl ketones, which are brominated by purified bromoperoxidase and then decay to form brominated methanes. However, whether similar acceptors also exist in brown or other red seaweeds is not known and other pathways may exist.

The brown seaweed *A. nodosum* (knotted wrack), which grows in large quantities in the North Atlantic and western Russian polar seas (*18*), contains two vanadium bromoperoxidases (*19*). One is located inside the so-called fruiting bodies and its presence shows a seasonal cycle (*6*). The other enzyme is located on the surface of the fruiting bodies and may be extracellular (*19*). This raises the interesting possibility that these seaweeds also release free hypobromous acid and bromine in seawater. Reaction of these bromine species with dissolved organic matter in seawater may well result in the formation of bromoform and other brominated compounds, and thus the origin of bromoform may be an indirect result of the formation of HOBr by seaweeds. In fact, Sauvageau (*20*) already re-

 0013-936X/91/0925-0446$02.50/0